Malaysian Journal of Chemistry, 2017, Vol. 19(1), 59 – 66

Aqueous Uranium Activity Removal by $CoFe_2O_4$ Nanoparticles

Tran Quang Dat*, Vu Dinh Thao, Pham Thanh Hung and Do Quoc Hung
Le Quy Don University of Technology, 236 Hoang Quoc Viet Street,
Cau giay District, Hanoi, Viet Nam
*Corresponding author: (e-mail: dattqmta@gmail.com)

Cobalt ferrite ($CoFe_2O_4$) nanoparticles have been prepared by the method of spraying-co-precipitation. The advantages of this approach are high productivity, excellent repeatability and high magnetic performances of the fabricated materials. The obtained materials were characterized by different techniques as X-ray diffraction, transmission electron microscopy, scanning electron microscopy. It was shown that $CoFe_2O_4$ has the face-centered cubic trevorite structure and particle size of about 18 nm. The vibrating sample magnetometer measurement had shown that obtained material had saturation magnetization of about 40 emu/g, remanences was 14 emu/g, and coercive forces (Hc) was 0.9 kOe. An investigation of uranium adsorption onto $CoFe_2O_4$ magnetic nanoparticles was studied in this research. This was confirmed by our experimental results using the method of inductively coupled plasma mass spectrometry. The pH effect, adsorption kinetics, and adsorption isotherms were examined in batch experiments. The sorption isotherm agreed well with the Langmuir model, having a maximum sorption capacity of 53.36 mg/g at pH = 6 and T = 298 K. Present research might eventually lead to a simple and low-cost method for fabricating magnetic materials and application for efficient removal of uranium from aqueous solution.

Key words: Nanoparticles; adsorption uranium; co-precipitation; $CoFe_2O_4$; isotherm models

Received: June 2016; Accepted: May 2017

Water is one of the most significant resources for life on the Earth but most of it is facing serious contamination due to various human activities. To remove colour, odour, inorganic and organic pollutants, adsorption, as an essantial technology in separation and purification procedures, is widely used in the water treatment industry. Compared with other techniques, such as membrane filtration, chemical oxidation, solvent extraction, ion exchange, photocatalysis, adsorption is a reliable perspective because of its simplicity, high efficiency, and low cost. Much effort has been focused on the development of novel adsorbing materials, including zeolitic imidazolate frameworks, metal organic frameworks, engineered carbons and magnetic materials [1,2].

As a naturally occurring element, uranium exists at low levels within soils, rocks, sediments, underground water and sea water [3]. In the past decades, many cases of environmental contamination have resulted from overuse of uranium at industrial and military sites [4]. Uranium exists in t alsolution as aqueous uranyl (UO_2^{2+}) which is strongly adsorbed onto clay minerals and metal oxides under appropriate conditions. However, carbonate dissolved in solution can affect the nature of uranium and its mobility, which in turn affects its adsorption onto the materials. Wazne *et al.* [5] researched carbonate effects on hexavalent uranium adsorption by iron oxyhydroxide. They concluded that at pH>6 carbonate negatively affects U(VI) adsorption onto ferrihydrite. Zeta potential measurements demonstrated that U(VI) was adsorbed as a cationic species without carbonate and as anionic U(VI) complexes in the presence of carbonate at neutral pH. Consequently, we should not ignore the role of carbonate when discussing the adsorption of uranium.

Several methods have been developed to obtain ferrite particles, including the use of sonochemical reactions, mechanochemical synthesis, hydrolysis of precursors, thermal decomposition, aqueous co-precipitation, and hydrothermal synthesis. With regard to cobalt ferrite, the incorporation of cobalt ions leads to an increase of coercivity, which is due to the coupling of the spins between cobalt and iron ions. Moreover, with a large magnetocrystalline anisotropy constant ($k>10^5$ J/m^3), $CoFe_2O_4$ is regarded as a hard magnetic material [6].

Recently, ferrites have been employed in water purification. The majority of magnetic adsorbent materials do not change in their magnetic properties upon adsorption; additionally, the unique response of magnetic nanoparticles to adsorbates allows them to serve as self-indicating adsorbents. [7]

In our previous paper [8], we reported on the development of a productive method for obtaining $Zn_{0.5}Ni_{0.5}Fe_2O_4$ nanoparticles — the method of spraying-co-precipitation. The peculiarity of this method is that the solutions containing precursors are fed into the container-reactor in the form of a powerful flow of microscopic drops. Thanks to this, the developed technological method can provide high productivity, stability and reproducibility for obtaining ferrite nanoparticles with relatively uniform size.

In the present work, we tried to apply the developed technological method for fabrication of cobalt ferrite nanoparticles and to investigate the ability of the obtained nanomaterial to extract uranium ions from the aqueous medium. Attempts were made to clarify the optimal recovery conditions of uranium on $CoFe_2O_4$ adsorbent as a function of pH, contact time as well as the equilibrium concentration of uranium. Isotherm models are proposed to explain the sorption characteristics of $CoFe_2O_4$.

EXPERIMENTAL

Materials

Analytical grade chemicals were used. Cobalt(II) nitrate hexahydrate (Co(NO3)2.6H2O, 99%), iron(III) chloride hexahydrate (FeCl3.6H2O, 99%), sodium hydroxide (NaOH, 99%) and nitric acid (HNO3, 65%) were supplied by Merck, Germany. Uranium stock solution was prepared by dissolving appropriate amount of UO2(NO3)2.6H2O (Sigma-Aldrich) in water. All solutions were prepared with double distilled water.

Synthesis of $CoFe_2O_4$

$CoFe_2O_4$ nanoparticles were prepared by the method of spraying-coprecipitation [8]. Initially, a mixed liquid of $Co(NO_3)_2$ 0.1 mol/l, and $FeCl_3$ 0.2 mol/l was contained in a pressure vessel. One other pressure vessel contain 0.8 mol/l solution of NaOH. A 3 atm compressed air flow should be piped into the two vessels so that the liquid comes out in the mist form at the nozzles. Spray speed at the two nozzles was similar at 0.2 l/min. Co-precipitation reaction happen at the larger vessel, containing NaOH 10^{-4} mol/l to the keep the reaction environment at the constant pH = 10. The precipitate was collected, filtered and washed thoroughly until the pH reached 7–8. The precipitated slurry was dried at the temperature of 50°C, ground and then calcinated at 1000°C for 4 h. After calcination, the obtained powder was ground again before measurements. By the technological process described above, we had synthesized a large quantity of nanostructured $CoFe_2O_4$ material.

Characterization of Materials

The morphologies and crystal structures of the $CoFe_2O_4$ nanoparticles were characterised using field emission scanning electron microscopy (FE-SEM, HITACHI S4800), transmission electron microscopy (TEM, JEM-100CX instrument with an accelerating voltage of 80 kV) and X-ray diffraction (XRD, Bruker D8 with Cu $K_{\alpha 1}$ radiation $\lambda = 1.54056$ Å). Magnetic measurements were performed with a vibrating sample magnetometer (VSM, DMS 880 in magnetic fields up to 13.5 kOe).

Adsorption Experiments

A batch technique was applied to study the sorption of uranium(VI) complex from the prepared solutions by $CoFe_2O_4$. Batch sorption experiments were carried out in a thermostated shaker bath. The temperature is maintained at 25°C. Typically, $CoFe_2O_4$ was dispersed in 50 ml solution containing various initial uranium concentrations at different pH values with different contact times. The pH was adjusted by adding 0.5 mol/l HNO_3 and 0.1 mol/l NaOH into the solution for each experiment. At the end of the adsorption period, $CoFe_2O_4$ was separated from the solution by magnetic separation, and the effluent was analyzed by inductively coupled plasma mass spectrometry

(ICP-MS, Agilent 7500). The amount of the uranium loading (mg) per unit mass of $CoFe_2O_4$ was obtained by:

$$Q_{eq} = \frac{C_0 - C_{eq}}{m} V$$

Where, Q_{eq} (mg/g) is adsorption capacity, C_0 and C_{eq} (mg/l) are the initial and equilibrium concentrations of uranium (VI) solution, m is the weight of sorbent (g), V is the volume of the uranium(VI) solution (l).

RESULTS AND DISSCUSSION

Morphology and Formation of Nanoparticles

Figure 1 shows the TEM image of the slurry obtained after spraying. It indicates that the as-synthesized material is of very small size, about just several nm. The SEM image of nanoparticles is shown in Figure 2. SEM image of the as-synthesized samples exhibited uniform, almost spherical shaped and loosely agglomerated particles of $CoFe_2O_4$ ferrite nanoparticles.

To analyze the $CoFe_2O_4$ particle size distribution, we selected the most clear-cut particles in Figure 2 to determine the particle dimensions and then compiled the particle size distribution diagram. The results are shown in Figure 3. In this figure, one can see that the particle sizes range from 12 to 24 nm in diameter. The distribution curve has a normal bell-shape with the maximum in the region of 18 – 19 nm.

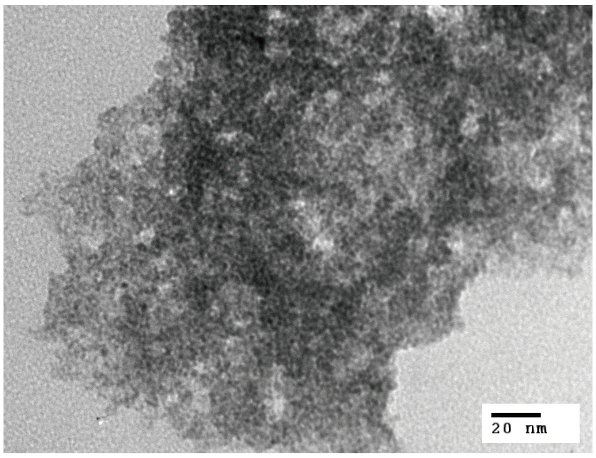

Figure 1. TEM image of $CoFe_2O_4$ slurry.

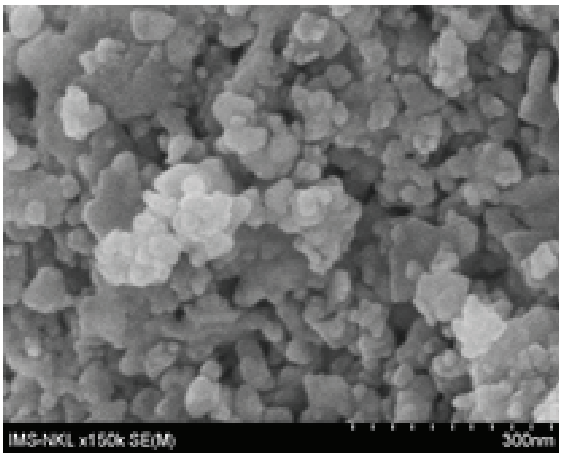

Figure 2. SEM image of $CoFe_2O_4$ nanoparticles.

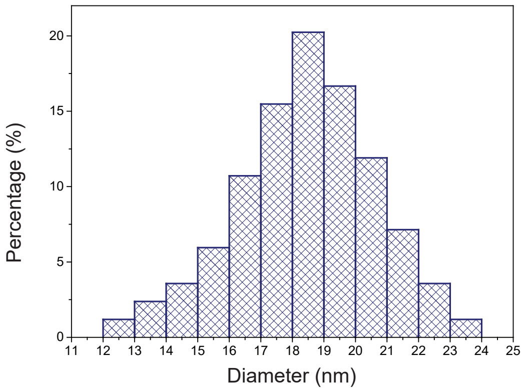

Figure 3. Particle size distribution of $CoFe_2O_4$.

Figure 4 shows the XRD patterns of the $CoFe_2O_4$ nanoparticles. The broad and well defined diffraction peaks were observed at 2θ = 30.18, 35.54, 43.14, 53.52, 57.18, 62.66 degrees, corresponding to (220), (311), (400), (422), (511) and (440) planes, respectively. X-ray diffraction data identified that the sample had face-centered cubic trevorite structure. The estimated value of lattice constants was found to be a = 8.377 Å. The value of crystallite size of the $CoFe_2O_4$ nanoparticles was evaluated by fitting the width of (311) reflection using Scherrer formula $d = k\lambda/\beta.\cos\theta$, where k is equal 0.94, λ is the X-ray wavelength, β is the peak full width half maxima and θ is the diffraction peak position. The estimated value of crystallite size of the material was found to be about 18 nm. This result was in good agreement with the previous analysis of the SEM image.

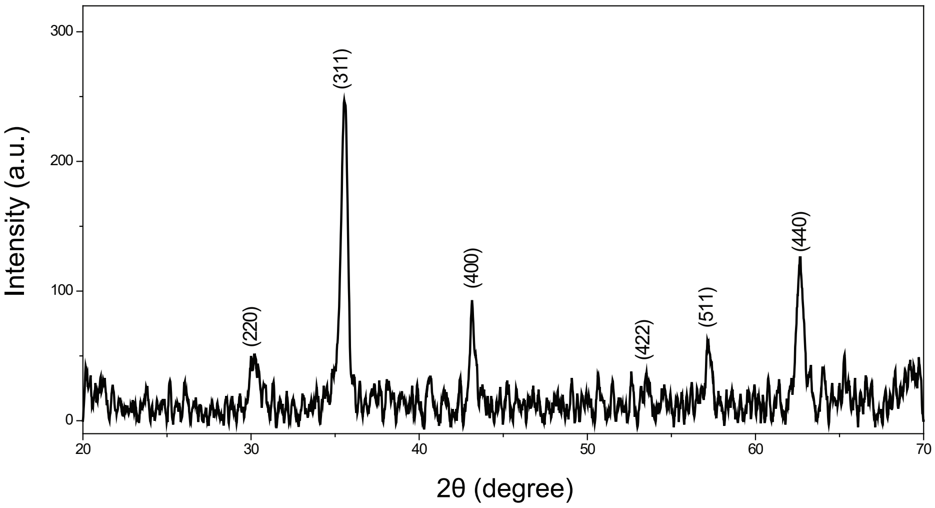

Figure 4. XRD patterns of $CoFe_2O_4$.

Magnetization Measurement

Room temperature magnetization for compositions of $CoFe_2O_4$ was investigated and is shown in Figure 5. Magnetic hysteresis loops were observed in two band magnetic fields: from –1 kOe to 1 kOe [in Figure 5(a)] and from –13.5 kOe to 13.5 kOe [in Figure 5(b)].

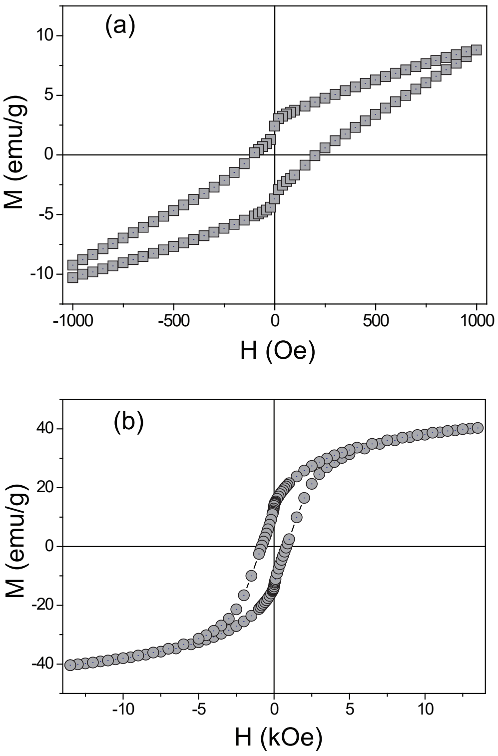

Figure 5. Room temperature magnetic hysteresis loops of the $CoFe_2O_4$ nanoparticles (a) in weak magnetic field; (b) in strong magnetic field.

The magnetization of $CoFe_2O_4$ nanoparticles increased with external magnetic field strength, however, it did not reach the saturate state yet under a magnetic field of 13.5 kOe. The VSM measurement showed that obtained material was ferrite with saturation magnetization (Ms) of about 40 emu/g, remanences (Mr) was 14 emu/g, and coercive forces (Hc) was 0.9 kOe. Precisely, as expected for a system of magnetic nanoparticles the magnetization did not saturate but reached a maximum value of about 40 emu/g for the maximum applied field of 13.5 kOe. A large saturation magnetization mades this adsorbent easy to separate from solution by applying an external magnetic field.

Effect of Contact Time on Uranium Sorption

Figure 6 presents the amount of uranium sorption on $CoFe_2O_4$ nanoparticles as a function of contact time. It was evident that equilibrium was established after 60 min, and that further increase of the contact time did not influence the sorption process. From the figure, it could be seen that the sorption process had two distinctive stages, initial fast process completing in approximately 30 – 60 min followed by a slow and marginal uptake extending to several hours. Results of the sorption experiments indicated that magnetic nanoparticles were effective in decreasing the uranium concentration in the effluent. A maximum of 89.4% decreased from the initial concentration of 20 mg/l was observed during 240 min of contact time.

Similarly, two stages kinetics for uranium sorption on magnetic were reported, where the initial fast process was attributed to the adsorption of U(VI) ions on the surface and the slow process was due to the gradual reduction of uranium from solution [9]. To ensure that equilibrium was established in each case, a contact time of 60 min was selected for all batch adsorption experiments.

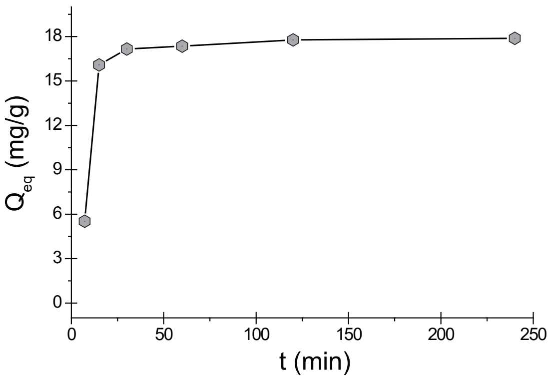

Figure 6. Effect of contact time on uranium sorption (Volume = 50 ml, nanomaterial = 50 mg, c_0 = 20 mg/l, pH = 6, t = 298K).

The adsorption data were treated according to the pseudo-first-order or pseudo-second-order kinetic equation [10, 11] to investigate the controlling mechanism of the adsorption process. As seen from Figure 7(b), the pseudo-second-order equation fitted well with the experimental data, and the correlation coefficient obtained for pseudo-second order equation was 0.998. Furthermore, the sorption capacities calculated by the pseudo-second-order model are very close to the experimental values. These results suggested that a pseudo-second-order sorption was a predominant mechanism.

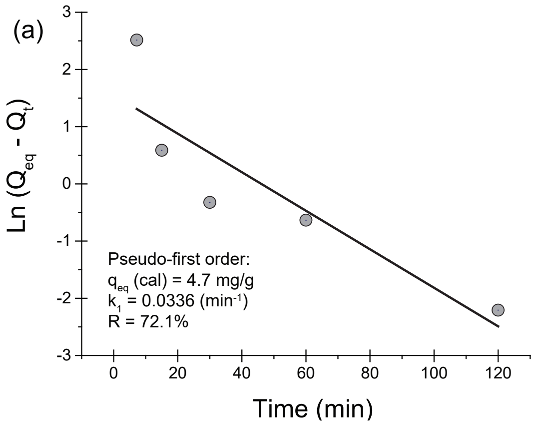

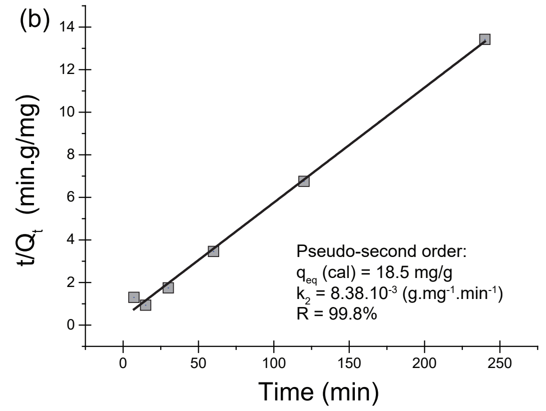

Figure 7. Pseudo-first (a) and second-order (b) plot for the sorption of uranium.

Effect of Initial pH

pH is one of the most important parameters affecting ion sorption. Influence of pH on adsorption was given in Figure 8 for 50 mg $CoFe_2O_4$ and 50 ml of 50 mg/l uranium(VI) solution at 298 K for 120 min, in the pH range of 4 – 10.

The removal of uranium sharply increased from 21.79 mg/l to 23.34 mg/l when the pH increases from 4 to 6. The maximum adsorption yield was observed at pH = 6. In acidic conditions, the adsorption process was not favoured because the surface of adsorbent was positively charged; UO_2^{2+} adsorbed was also positive. Moreover, excess H^+ occupied many adsorption sites. With a pH higher than 6, uranium was present as anionic species. With the increasing of the concentration of hydroxyl, dissolved carbonate and bicarbonate anions, the uranyl ion formed stable complexes with hydroxyl and carbonate like $UO_2(CO_3)_3^{4-}$, $UO_2(OH)_3^{4-}$ and $UO_2(CO_3)(OH)_3^-$ etc., which led to a slight decrease in the removal efficiency [12, 13]. This value of pH is also observed in previous reports about cobalt ferrite [9]. Consequently, pH 6 is considered as the optimum pH for further experiments.

Adsorption Isotherms

To find out the effect of equilibrium uranium concentration on the sorption process, experiments were conducted by varying the initial concentration of uranium from 5 to 150 mg/l. Figure 9 illustrates the amount of sorbed uranium on the magnetic nanoparticles after 60 min of equilibration. To account for the precipitation of uranium at the experimental pH, parallel experiments were conducted without $CoFe_2O_4$ nanoparticles. The results revealed that the precipitation of uranium species was insignificant even at the highest uranium concentration employed in our studies. Thus the removal of uranium in the presence of magnetic could be assigned to the interaction between magnetic surface and uranium species present in solution. Under our experimental condition, uranium loading onto the nanoparticles was found to be saturated at approximately 50.2 mg/g of the nanoparticles.

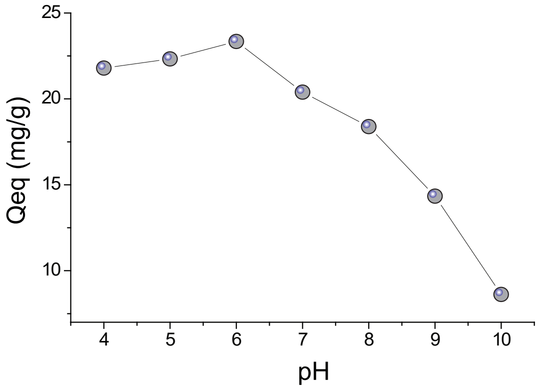

Figure 8. Effect of pH on sorption of uranium (Volume = 50 ml, nanomaterial = 50 mg, C_0 = 26 mg/l, T = 298K).

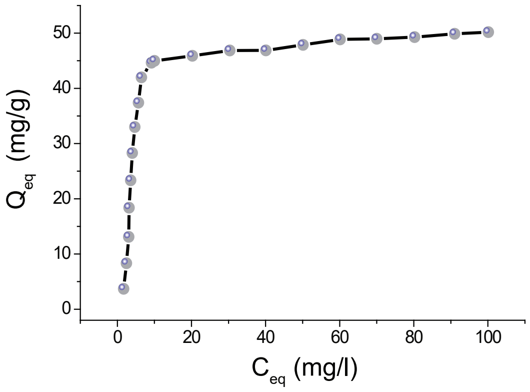

Figure 9. Effect of equilibrium uranium on the sorption on $CoFe_2O_4$ nanoparticles (Volume = 50 ml, nanomaterial = 50 mg, pH = 6, time = 60 min, T = 298K).

To understand the adsorption behaviour of the adsorbents, the equilibrium data were evaluated according to the Langmuir, Freundlich isotherm and Dubinin–Radushkevich models [14–16]. The linear plots of Langmuir, Freundlich, and Dubinin – Radushkevich equations representing uranium(VI) sorption are illustrated in Figure 10. The corresponding Langmuir, Freundlich and Dubinin – Radushkevich parameters, along with the correlation coefficients, are reported in Table 1.

The Langmuir model appeared to be the best fitting model for uranium(VI) sorption with a high correlated coefficient R^2 (0.993). According to the Langmuir isotherm, monolayer saturation capacity of $CoFe_2O_4$ was about 53.36 mg/g for uranium(VI) at 298K.

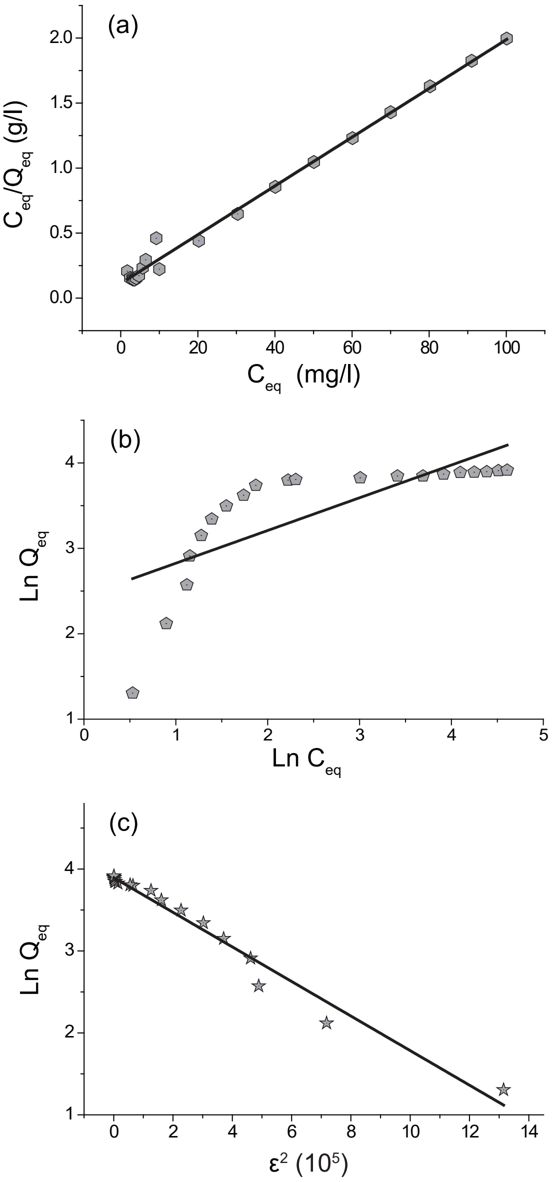

Figure 10. Comparison of the model fits of Langmuir (a), Freundlich (b) and Dubinin – Radushkevic (c) isotherms for the removal of uranium(VI) by $CoFe_2O_4$, pH = 6, T = 298K.

Table 1. Isotherm constants for the sorption uranium(VI) onto $CoFe_2O_4$.

Parameter		Value	R^2
Langmuir:	Q_m (mg/g)	53.36	0.993
	K_L (l/mg)	0.166	
Freundlich:	K_F (l/g)	11.5	0.543
	N	2.61	
D – R:	$K_{D\text{-}R}$ (mol^2J^{-2})	$2.11.10^{-6}$	0.975
	Q_m (mg/g)	49.1	

CONCLUSION

$CoFe_2O_4$ ferrite nanomaterial with the average size of 18 nm was successfully prepared by spraying-co-precipitation method. VSM measurements have shown that obtained material has saturation magnetization (Ms) of about 40 emu/g, remanences (Mr) was 14 emu/g, and coercive forces (Hc) was 0.9 kOe. Experimental results showed that the maximum sorption capacity of uranium with $CoFe_2O_4$ nanoparticles was 53.36 mg/g at pH = 6 and T = 298K. These unique magnetic properties of $CoFe_2O_4$ nanoparticles made it easy to collect them, for example, by using permanent magnets for consequent uranium desorption and then reuse of the adsorbent. So, $CoFe_2O_4$ was a promising adsorbent material to remove toxic and radioactive uranium(VI) from aqueous solutions.

ACKNOWLEDGEMENTS

This work was completed with financial support from the Le Quy Don Technical University, Vietnam (No.13.0.A.02).

REFERENCES

1. Banerjee, R., Phan, A., Wang, B., Knobler, C., Furukawa, H., O'Keeffe, M. and Yaghi, O.M. (2008) High-throughput synthesis of zeolitic imidazolate frameworks and application to CO_2 capture, *Science*, **319**, 939–943.
2. Glover, T.G., Dunne, I.K.I., Davis, R.J. and LeVan, M.D. (2008) Carbon–silica composite adsorbent: characterization and adsorption of light gases, *Microporous Mesoporous Mater,* **111**, 1–11.
3. Lovley, D.R., Phillips, E.J.P., Gorby, Y.A., Landa, and E.R. (1991) Microbial reduction of uranium, *Nature*, **350**, 413–416.
4. Bhalara, P. D., Punetha, D. and Balasubramanian, K. (2014) A review of potential remediation techniques for uranium(VI) ion retrieval from contaminated aqueous environment, *J. Env. Chem.*, Eng., **2(3)**, 1621–1634.
5. Wazne, M., Korfiatis, G.P. and Meng, X. (2003) Carbonate effects on hexavalent uranium adsorption by iron oxyhydroxide, *Environ. Sci. Technol*., **37**, 3619–3624.
6. Qing, S. and Zhang, Z.J. (2012) Controlled synthesis and magnetic properties of bimagnetic spinel ferrite $CoFe_2O_4$ and $MnFe_2O_4$ nanocrystals with core–shell architecture, *J. Am. Chem. Soc.*, **134**, 10182–10190.
7. Reddy, D.H.K. and Yun, Y.S. (2016) Spinel ferrite magnetic adsorbents: Alternative future materials for water purification?, *Coordination Chemistry Reviews*, **315**, 90–111.
8. Hung, D.Q. and Dat, T.Q. (2011) Large scale method to synthesize $Zn_{0.5}Ni_{0.5}Fe_2O_4$ nanoparticles with high magnetization, *VNU Journal of science Mathermatics-Physics*, **27(3)**, 160–164.
9. Tan, L., Liu, Q., Song, D., Jing, X., Liu, J., Li, R., Hu, S., Liu, L. and Wang, J. (2015) Uranium extraction using a magnetic $CoFe_2O_4$ graphene nanocomposite: kinetics and thermodynamics studies, *New J. Chem.*, **39**, 2832–2838.
10. López, F.A., Martín, M.I., Pérez, C., López-Delgado, A. and Alguacil, F.J. (2003) Removal of copper ions from aqueous solutions by a steel-making by-product, *Water. Res.*, **37**, 3883–3890.

11. Ho, Y.S. and McKay, G. (1999) Pseudo-second-order model for sorption processes, *Process Biochem.*, **34**, 451–465.

12. Sorg, T.J. (1991) Removal of uranium from drinking water by conventional treatment methods, in Radium and Uranium in Drinking Water, ed. C. Rebers, Lewis Publishers, Radon, p. 173.

13. Sprynskyy, M., Kowalkowski, T., Tutu, H., Cukrowska, E.M. and Buszewski, B. (2011) Adsorption performance of talc for uranium removal from aqueous solution, *Chem. Eng. J.*, **171**, 1185–1193.

14. Langmuir (1918) The adsorption of gases on plane surfaces of glass mica and platinum, *J. Am. Chem. Soc.*, **40**, 1361–1403.

15. Freundlich (1906) Uber die adsorption in losungen, *Z. Phys. Chem.*, **57**, 385–470.

16. Akar, T., Kaynak, Z., Ulusoy, S., Yuvaci, D., Ozsari, G. and Akar, S.T. (2009) Enhanced biosorption of nickel(II) ions by silica-gel-immobilized waste biomass: biosorption characteristics in batch and dynamic flow mode, *J. Hazard. Mater.*, **163**, 1134–1141.